Electronic Supplementary Information

High Surface Area Ordered Mesoporous $BiFeO_3$ Semiconductor with Efficient Water Oxidation Activity

Ioannis Papadas,[a] Joseph A. Christodoulides,[b] George Kioseoglou[a] and Gerasimos S. Armatas[a,]*

[a] *Department of Materials Science and Technology, University of Crete, Heraklion GR-71003, Crete, Greece*.

[b] *Naval Research Laboratory, 4555 Overlook Ave SW, Washington, DC 20375, USA.*

*E-mail: garmatas@materials.uoc.gr.

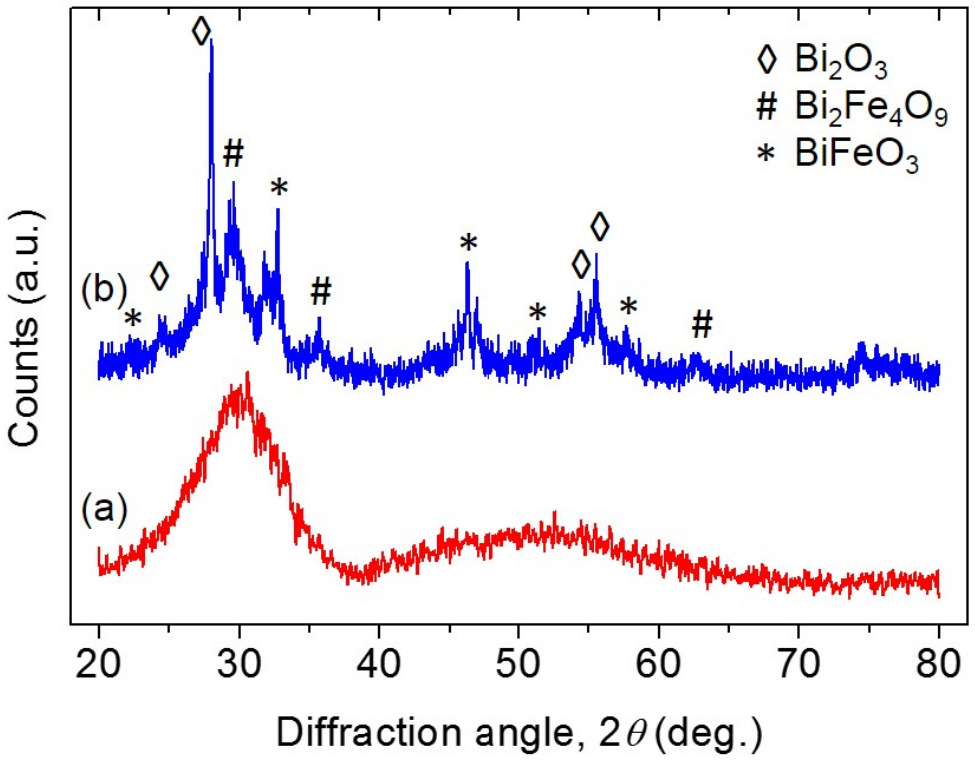

Fig. S1 XRD pattern of mesostructured frameworks casted from mesoporous CMK-3 carbon, (a) without using tartaric acid along with the $Bi(NO_3)_3$ and $Fe(NO_3)_3$ compounds and (b) using tartaric acid at a 0.5:1 molar ratio with respect to metal ions. The product in (b) is composed of crystalline Bi_2O_3, $Bi_2Fe_4O_9$ and $BiFeO_3$.

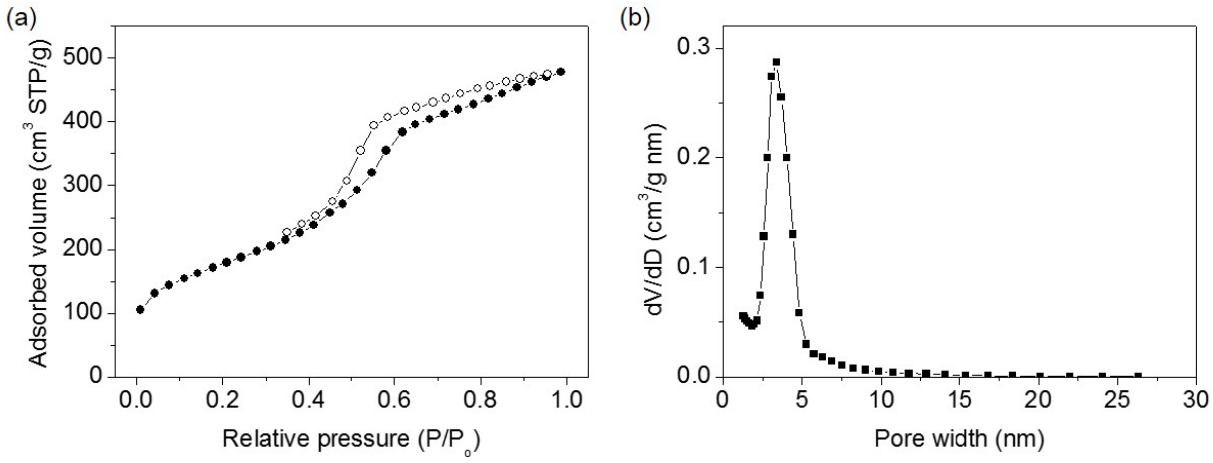

Fig. S2 (a) Nitrogen adsorption and desorption isotherms at 77 K and (b) the corresponding NLDFT pore size distribution for mesoporous CMK-3 carbon, indicating a mesopore size of 3.2 nm. Analysis of the adsorption data with the BET method gives surface area of 632 m^2g^{-1} and total pore volume of 0.73 cm^3g^{-1}. Given an estimation of the mesopore diameter (D_p) at 3.2 nm and the unit cell size (a_o) at 9.8 nm, the pore wall thickness (WT) is about 6.6 nm, according to the equation $WT=a_o-D_p$.

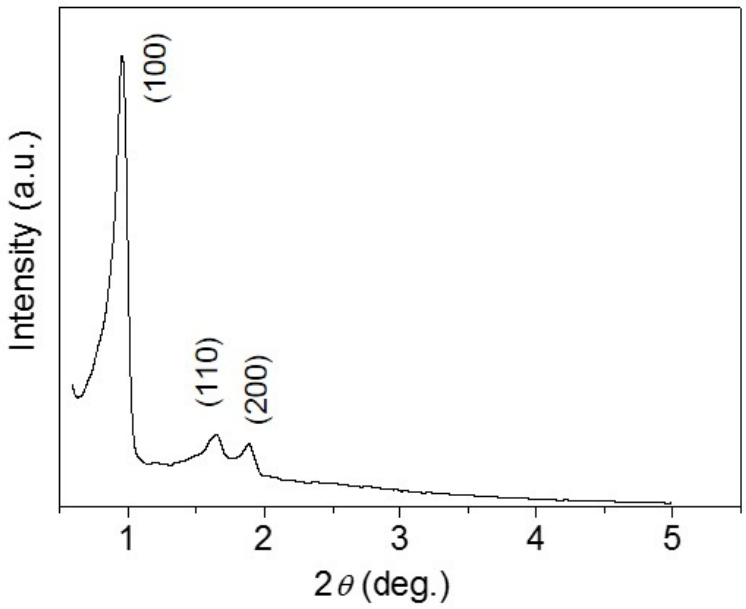

Fig. S3 Low-angle XRD pattern of mesoporous SBA-15 silica. The indexing of the Bragg diffractions is consisted with a hexagonal *p6mm* unit cell with lattice parameter a_o=10.7 nm.

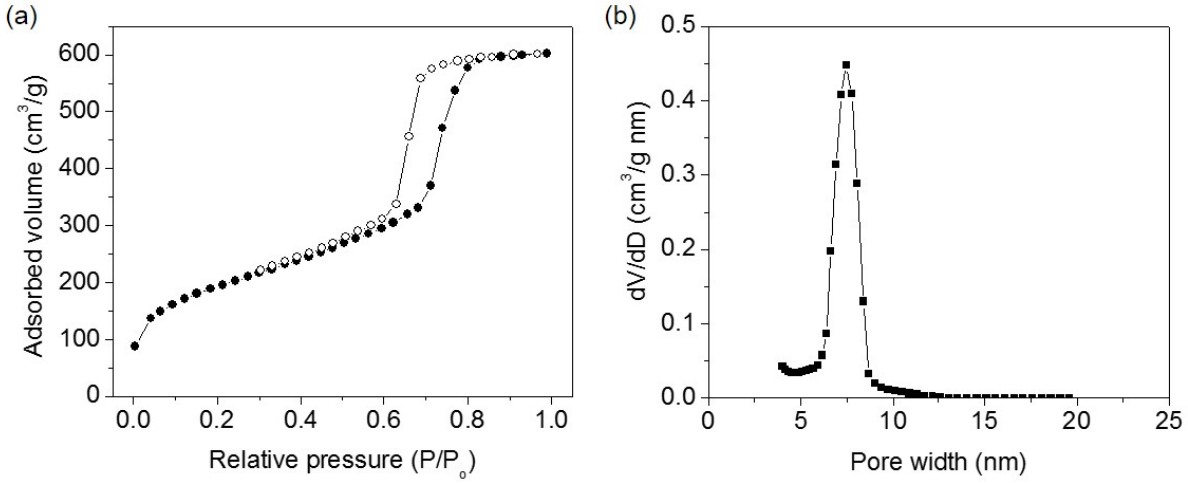

Fig. S4 (a) Nitrogen adsorption and desorption isotherms at 77 K and (b) the corresponding NLDFT pore size distribution for mesoporous SBA-15 silica, indicating a mesopore size of 7.8 nm. Analysis of the adsorption data with the BET method gives surface area of 650 m^2g^{-1} and total pore volume of 0.88 cm^3g^{-1}. Given an estimation of the mesopore diameter (D_p) at 7.4 nm and the unit cell size (a_o) at 10.7 nm (see Fig. S3), the pore wall thickness (WT) is about 3.3 nm, according to the equation $WT=a_o–D_p$.

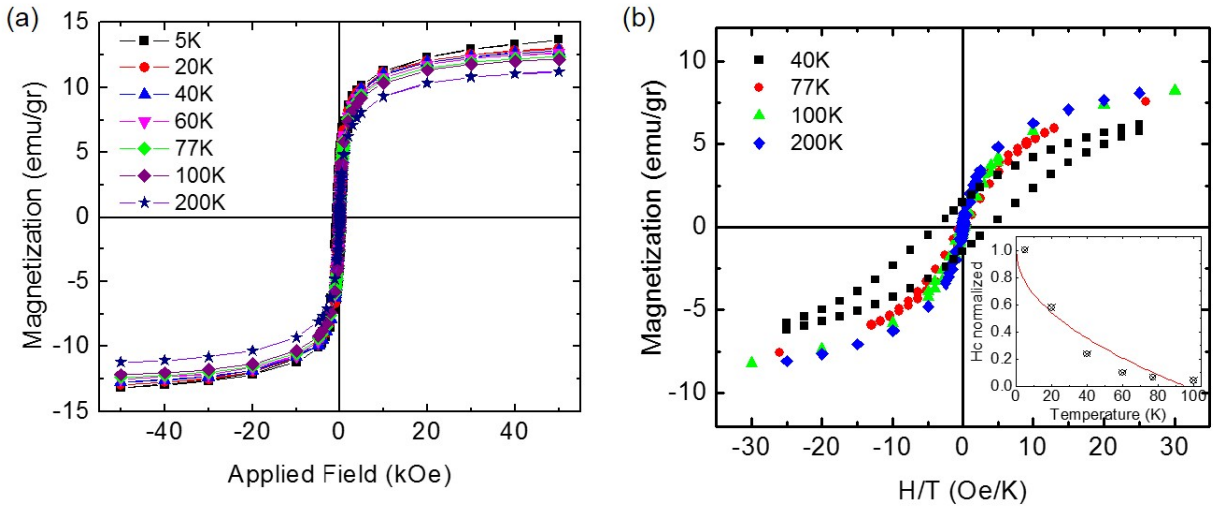

Fig. S5 (a) M-H loops at different temperatures for mesostructured $BiFeO_3$ in the -50 to +50 kOe range. Fast saturation of the magnetization is observed. (b) Magnetization plotted as function of H/T in the very narrow range of -35 to +35 Oe for 40, 77, 100 and 200 K. The inset shows the temperature dependence of the coercivity normalized to the value at 5 K. Black points are the experimental data and red line is root square dependence of the coercivity (H_C=1–$(T/T_B)^{1/2}$) assuming blocking temperature T_B = 95 K.

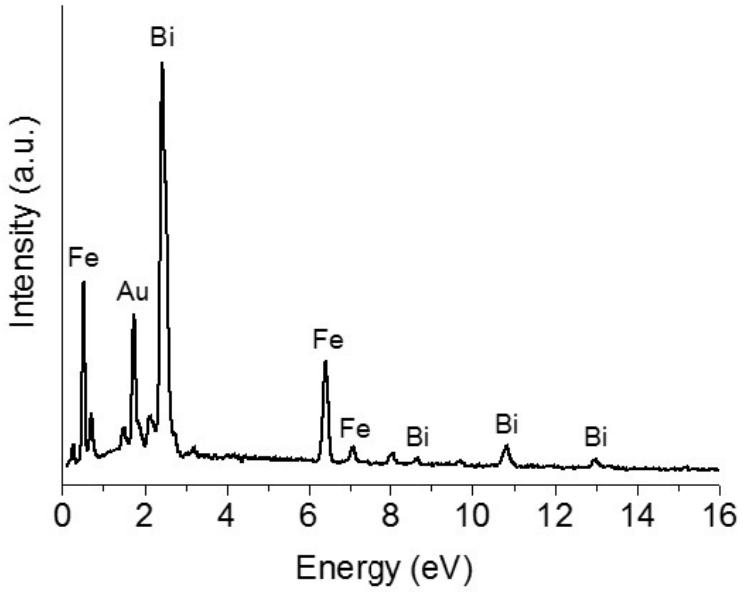

Fig. S6 Typical EDS spectrum for mesoporous Au/$BiFeO_3$ photocatalyst. The EDS analysis indicates an average atomic ratio of Au/Bi/Fe ~0.8:49.7:49.5 that corresponds to a ~1 wt % Au loading.

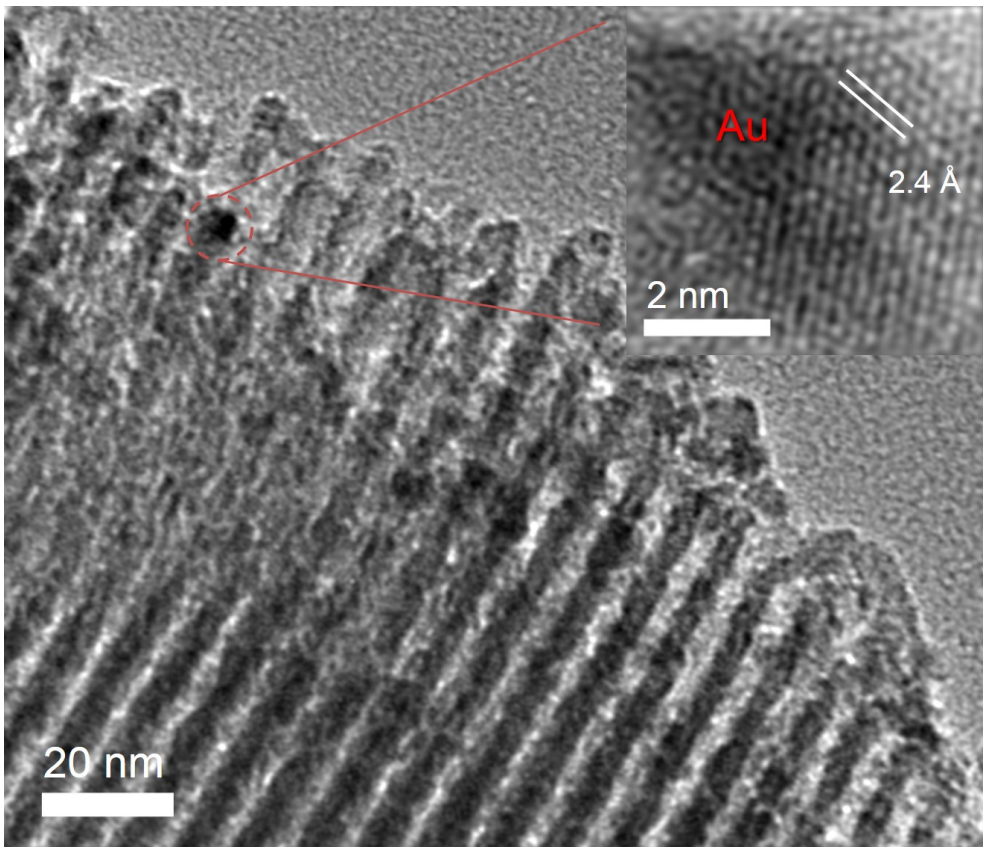

Fig. S7 Typical TEM image of mesoporous Au/$BiFeO_3$ sample. The inset shows the HRTEM image of an individual Au nanoparticle. The measured *d*-spacing is around 2.4 Å which is in consistent with the Au (111) crystal plane.

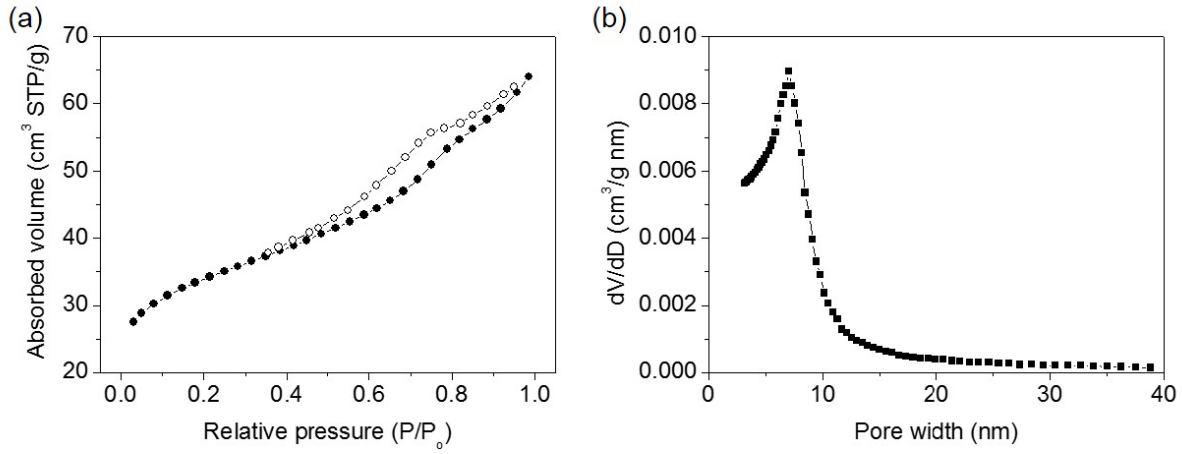

Fig. S8 (a) Nitrogen adsorption and desorption isotherms at 77 K and (b) the corresponding NLDFT pore size distribution for mesoporous Au/$BiFeO_3$ photocatalyst. Analysis of the adsorption data with the BET method gives surface area of 116 m^2g^{-1} and total pore volume of 0.10 cm^3g^{-1}. The NLDFT analysis of the adsorption data indicates a mesopore size of 7.0 nm.

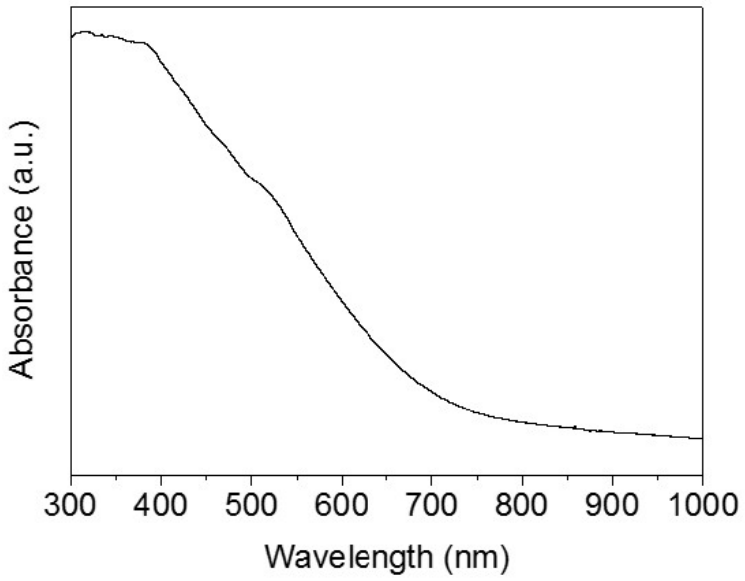

Fig. S9 UV-Vis/NIR absorption spectrum of mesoporous Au/$BiFeO_3$ heterostructure.

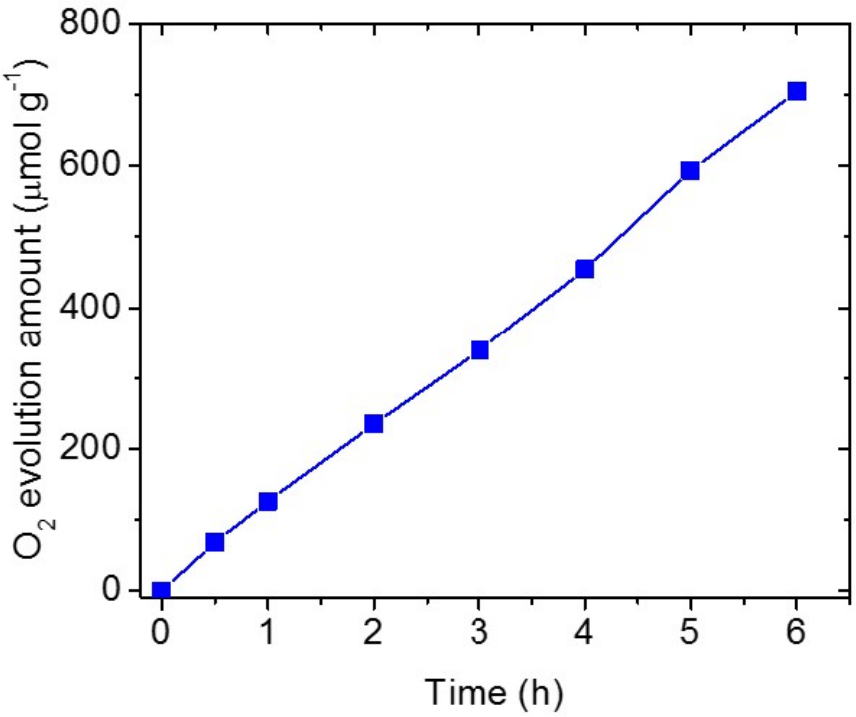

Fig. S10 Oxygen evolution profile for mesoporous Au/$BiFeO_3$ under visible ligth irradiation, showing a O_2 evolution rate of ~120 μmol h^{-1} g^{-1}.